

Article

An Analytical Expression for the Fundamental Frequency of a Long Free-Spanning Submarine Pipeline

Ty Phuor ¹, Pavel A. Trapper ² and Avshalom Ganz ^{1,*}¹ Department of Civil Engineering, Ariel University, Ariel 40700, Israel² Department of Civil and Environmental Engineering, Ben-Gurion University of the Negev, Beer-Sheva 84105, Israel; trapper@bgu.ac.il

* Correspondence: aganz@ariel.ac.il

Abstract: The DNVGL-RP-F105 guidelines provide essential techniques for the preliminary design of undersea pipelines. However, its approximations for static displacement and the natural frequency of the pipe are restricted to cases where the ratio of the pipe's diameter to its length (L/D) is less than 140. This limitation poses challenges for longer spans, which, although rare, can sometimes be unavoidable. This study introduces a novel analytical method, rooted in the energy method and cable theory, for computing the static deformation and natural frequency of long free-span underwater pipelines. We conducted a comprehensive verification of our proposed method by comparing its outcomes with those of 212 finite element analysis simulations. The results reveal excellent predictions for long spans. However, for shorter spans, traditional methods remain more accurate. Additionally, we explored the influence of pipeline's diameter, thickness, and boundary conditions on both static displacement and frequency, providing valuable insights for design considerations. We found that the boundary conditions' impact on the fundamental frequency becomes negligible for long spans, with up to a 10% difference between pinned–pinned and fixed–fixed conditions. In essence, this research offers a vital enhancement to the existing DNV guidelines, becoming particularly beneficial during the preliminary design phases of pipelines with L/D ratios exceeding 140.

Keywords: free spanning; submarine pipeline; buoyancy; natural frequency; static deformation; vortex-induced vibration (VIV)

MSC: 74H10

Citation: Phuor, T.; Trapper, P.A.; Ganz, A. An Analytical Expression for the Fundamental Frequency of a Long Free-Spanning Submarine Pipeline. *Mathematics* **2023**, *11*, 4481. <https://doi.org/10.3390/math11214481>

Academic Editors: Wei Zhang, Yuxin Hao and Youhua Qian

Received: 10 September 2023

Revised: 5 October 2023

Accepted: 9 October 2023

Published: 30 October 2023



Copyright: © 2023 by the authors. Licensee MDPI, Basel, Switzerland. This article is an open access article distributed under the terms and conditions of the Creative Commons Attribution (CC BY) license (<https://creativecommons.org/licenses/by/4.0/>).

1. Introduction

Submarine pipelines are an indispensable component of the oil and gas industry [1–4], and are the primary mode of transporting hydrocarbon products from offshore wells to onshore processing facilities and end-users [5–8]. Compared to other transportation modes, such as tanker ships [9–11], submarine pipelines are a cost-effective solution for the transportation of oil and gas [12–15]. Submarine pipelines may be in various diameters, with small-diameter pipelines usually employed for transporting hydrocarbon products from manifold to manifold, or from manifold and wellhead to the platform. In contrast, large-diameter pipelines are commonly used for transporting products from the platform to the shore. These pipelines can stretch over thousands of kilometers, making them a crucial component of the oil and gas industry. During the installation stage, harsh seabed conditions or budget constraints may prevent submarine pipelines from being buried below the ground. As a result, they may be subjected to free spans, which can arise due to the unevenness of the seabed, erosion of the seabed, pipeline crossings, and tie-ins to other structures [16,17]. For instance, free-spanning pipelines, due to the roughness of the seafloor, can be distinguished as single free-span and multiple free-span pipelines [1–8].

From an engineering point of view, one of the more widely recognized root causes of structural pipeline collapse is a free span in which the unsupported pipeline becomes very vulnerable, due to (1) being over-stressed by the pipe's self-weight and its contents [15,18,19] and (2) vortex-induced vibration-based fatigue from the current varying with time [20–23]. In this sense, if the free span cannot be avoided, it is important to determine the maximum allowable length and justify the actual free span accordingly. Consequently, many researchers and practical engineers have performed studies to justify the length of free-span pipelines in order to guarantee their safety by providing a reliable free-span design. For example, DNVGL-RP-F105 Sect. 6.8 [24] recommends that a lengthy free-span pipeline might be justified by installing grout bags, sandbags, mechanical rigid supports, etc. However, it is clearly noted that the aforementioned measures employed to justify these excessive span lengths become unachievable and very costly if the pipeline is laid in deep and very deep water depths (i.e., 1500 to 2000 m) by lying over a submarine valley [25,26]. Consequently, the stability issue of free-spanning pipelines has become a potential study area for all oil and gas industries. Therefore, studies have revealed that when a current flows across a pipeline, it forms vortex shedding in two ways at low-flow velocities, and symmetric and asymmetric vortex shedding at high velocities [25,26].

More precisely, the vortices of the cross-section of a free-span pipeline can be observed as symmetrical and asymmetrical vortices that, respectively, produce the in-line vibration along the flow direction and simultaneously the in-line and the cross-flow vibrations with the parallel and perpendicular to the flow directions [25,26]. In addition, it is observed that in-line impulses occur in the in-line direction, while cross-flow impulses occur in the perpendicular direction. Thus, the in-line excitation at a frequency can be twice compared to that of cross-flow excitation and, consequently, it has a smaller stress and motion amplitude [27]. From an engineering perspective, it is noted that the synchronization of vortex shedding or the resonance phenomenon can occur when the vortex shedding frequency, which is the frequency of the hydrodynamic forces governed by the flow velocity, the pipe's outer diameter, and Strouhal's number, is close to the natural frequency of the free-spanning pipeline [12,28–34]. Consequently, if the pipeline starts to resonate, significant deformation and severe stress can occur, leading to potential collapse.

Consequently, to ensure the safety and stability of a free-spanning pipeline, it is essential to compute its natural frequency to determine the vibration amplitude and cyclic stresses. Numerous studies have been conducted to compute the natural frequency, with a focus on the fundamental frequency, which is the first mode of frequency and is important for computing the reduced velocity to observe the structure's stability [12,26,35]. For instance, Palmer and King [12] developed a closed-form solution to compute the frequency based on a linear elastic beam with no axial force, while Xiao and Zhao [26] proposed a simplified equation that considers the boundary condition factors and the axial forces for a free-spanning pipeline with a maximum span of 50 m. The authors concluded that the frequency increases and decreases with the tensile and compressive axial forces, respectively. In addition, Yaghoobi et al. [35] suggested a closed-form solution to calculate the frequency of offshore pipelines with a free span of up to 80 m by taking into account seabed soil characteristics, and found that the soil type has a strong influence on the frequency, as the frequency increases with the increase in the soil stiffness. Nevertheless, Sarkar and Roy [36] performed parametric studies for computing the frequencies with various magnitudes of parameters (i.e., thickness, diameter, span length, and homogeneous soil stiffness) up to a maximum free span of 100 m using the finite element method and the DNVGL-RP-F105 [24] guidelines. Additionally to these, Sarkar and Roy [37] also determined the frequency by considering the nonhomogeneous soil stiffness using Abaqus. Last but not least, DNVGL-RP-F105 [24], which is the design guideline for free-spanning offshore pipelines used by the most dominant oil and gas industries, developed an empirical equation for computing the frequency by including the effects of the static deformation of the pipe, axial forces, and the stiffness of the supporting soil. However, it is observed that all studies mentioned above compute the natural frequency of the free-spanning pipeline, which is limited to the ratio

$\frac{L}{D} \leq 140$ [24], where L is the length of the free span and D is the diameter of the pipe, owing to the unreliable computed deformation of the pipe for $\frac{L}{D} > 140$. Moreover, it is worth stating that, for some applications, a long free-spanning pipeline will be necessary to cross over a submarine valley or a canyon [25]; consequently, the length of the free span might reach 500 m, and the gap between the pipeline and the seabed might be up to 50 m [38].

In addition, for such long free-spanning pipes (i.e., $\frac{L}{D} > 140$), DNVGL-RP-F105 Sect. 6.8 [24] recommends employing the finite element method (FEM), which is widely recognized to be an effective method of solving geotechnical [39,40] and structural [41] engineering problems. In this sense, the three-dimensional (3D) FEM-based pipeline free span analysis is usually performed in Abaqus, Reflex, Offpipe, OrcaFlex, etc. [21,42,43]. However, in many simulations, the employment of these commercial finite element programs becomes frustrating and time-consuming in terms of model definition as well as data processing due to the burdensome Graphical User Interface (GUI) [16,44]. To elucidate this, the establishment and resolution of an FEM model can generally take hours and minutes, respectively. In contrast, closed-form solutions are nearly instantaneous. Therefore, a more convenient and time-saving approach may be represented by a simple closed-form solution for a preliminary design.

Therefore, this paper presents a new closed-form solution for computing reliable static deformation and the natural frequency of a long free-spanning submarine pipeline, using the energy method based on the uniform linear-elastic beam with only the axial effect in conjunction with the analytical solution produced by DNVGL-RP-F105 Sect. 6.8 [24]. Specifically, this study extends DNVGL-RP-F105 Sect. 6.8 [24] to compute the reliable frequency for $L/D \geq 140$. In addition, the purpose of this article is to fill the gap in the analytical expression used for computing the frequency of a long free-spanning pipeline with $L/D > 140$, which has never been reported in the literature, and is challenging due to the limited prior research, the inherent complexity of the problem, and the need for validation. Consequently, a verification of this study is also provided and discussed thoroughly by the comparison of the computed static displacement and frequency of the pipelines with those values calculated by the existing methods; and it is found to be in a reasonable agreement. This rigorous verification introduced an added layer of complexity, necessitating the creation of a specialized computational framework. This framework encompasses algorithms for both pre- and post-processing the FEM simulations automatically. It is worth noting that even though this proposed closed-form solution is simple and easy to implement, this solution has never been presented in the literature, in particular for a long free-span pipeline. Specifically, it should be noted that this solution only considers the axial force generated by the configuration form of a long pipeline and does not take into account external axial forces or those generated by pressure and temperature, which are outside the scope of this study. This limitation is discussed further in Section 2.

2. Methodology

2.1. Derivation of Deformation Profile of a Long Free-Spanning Pipeline

Logically, a long free-spanning pipeline can be considered a cable due to its configuration and shape. To determine its deformation, in this study, it is treated as a long cable, as shown in Figure 1. The figure presents a free-body diagram of an infinitesimal segment of a long free-spanning pipeline in equilibrium under a vertical load. Consequently, the equation of this long pipeline's profile can be derived as follows, where $T(x)$ is the axial force generated by the configurational shape of the pipeline (see Figure 1), $H(x)$ is the constant horizontal force ($y(x)$), v_1 and v_2 are the vertical forces at points 1 and 2, respectively, and q is the uniformly distributed load.

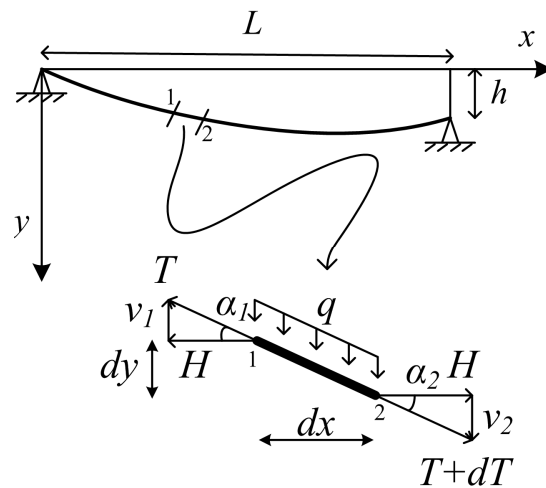


Figure 1. Free body of the infinitesimal segment of a long free-spanning pipeline at equilibrium under uniform load.

In relation to Figure 1, the equilibrium equation in the x direction can be written as

$$H = H + \frac{dH}{dx} \rightarrow H = \text{const} \tag{1}$$

$$\tan\alpha_1 = \frac{dy}{dx} = \frac{v_1}{H} = \text{slope at point 1} \tag{2}$$

$$\tan\alpha_2 = \frac{dy}{dx} + \frac{d^2y}{dx^2}dx = \frac{v_2}{H} = \text{slope at point 2} \tag{3}$$

and the forces of the equilibrium in the y direction can be written as

$$v_1 - qdx - v_2 = 0 \tag{4}$$

Extrapolating from Equations (1)–(3), Equation (4) becomes

$$\frac{d^2y}{dx^2} = -\frac{q}{H} \tag{5}$$

Therefore,

$$y = -\frac{q}{2H}x^2 + ax + b \tag{6}$$

By applying boundary condition at both ends with the same height, the coefficients a and b can be defined, as in Equation (7).

$$y_{x=0} = 0 \implies b = 0 \tag{7a}$$

$$y_{x=L} = h = 0 \implies a = \frac{qL^2}{2HL} \tag{7b}$$

Therefore, the equation of a long free-spanning pipeline profile is expressed as

$$y(x) = -\frac{q}{2H}x^2 + \frac{qL^2}{2HL}x \tag{8}$$

The deformation of the long pipeline is found to be highly influenced by the horizontal force H , which must be calculated using a simplified approach. To achieve this, a shallow and horizontal pipeline is assumed, as shown in Figure 2. Consequently, the cable’s slope angles are small, and therefore $T \approx H$. The force on the increment dx is $q \cdot dx$, and the work

done by the virtual displacement $y(x)$ is $q \cdot y(x) \cdot dx / 2$ (for quasi-static loading). Therefore, the virtual work performed by the complete pipeline can be written as Equation (9).

$$W = \int_0^L \frac{q \cdot y}{2} dx \tag{9}$$

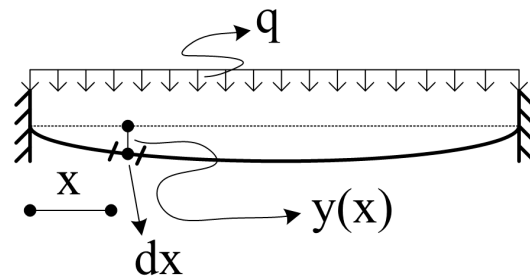


Figure 2. Long free-spanning inclined pipeline under uniform load.

Similarly, by considering only the axial effect, the strain energy of the pipeline can be expressed.

$$U = \frac{k}{2} \Delta L^2 \tag{10}$$

$$k = \frac{AE}{L} \text{ and } \Delta L = \frac{HL}{EA} \tag{11}$$

Therefore, Equation (10) becomes

$$U = \frac{H^2 L}{2EA} \tag{12}$$

By equating the work conducted on the system to the strain energy (see Equation (13)), the virtual work of the system can be expressed as in Equation (14). By substituting Equation (8) into Equation (14), the horizontal force in the case of uniformly distributed load is given as in Equation (15).

$$W = U \tag{13}$$

$$\int_0^L \frac{q \cdot y(x)}{2} dx = \frac{H^2 L}{2EA} \tag{14}$$

$$H = \sqrt[3]{\frac{q^2 EA}{12} L^2} \tag{15}$$

Therefore, Equation (8) can be rewritten as

$$y(x) = \frac{q}{2 \cdot \left(\frac{q^2 EA}{12} L^2\right)^{1/3}} x(L-x) \tag{16}$$

where E is the Young’s modulus, A is the cross-section area of the pipe, y is the pipe deformation, x is the distance along the pipeline, q is the uniformly distributed load of the pipe, and L is the total length of the pipe. It is noteworthy that even though this analytical expression is straightforward to apply, it has not been previously reported in the literature, particularly for a long free-span pipeline.

2.2. Determination of Natural Frequency of a Long Free-Spanning Pipeline

It is well-known that DNVGL-RP-F105 Sect. 6.8 [24] provides an equation (Equation (17)) that can be used to compute the frequency of a free-span pipeline.

$$f \approx C_1 \sqrt{\frac{EI}{m_e L_{eff}^4} \left(1 + \frac{S_{eff}}{P_{cr}} + C_3 \left(\frac{\delta}{D} \right)^2 \right) (1 + CSF)} \tag{17}$$

where $\delta = C_6 \frac{q_{sub} \cdot L_{eff}^4}{EI(1+CSF)} \left(\frac{1}{1 + \frac{S_{eff}}{P_{cr}}} \right)$ is the static deformation of the pipe.

It should be noted that the recommended practice (i.e., DNVGL-RP-F105 Sect. 6.8 [24]) provides an analytical solution for calculating the frequency of a free-spanning pipeline, but it is only applicable when the ratio of the pipe length over the pipe diameter is smaller than 140 (i.e., $\frac{L}{D} < 140$). For longer pipelines (i.e., $\frac{L}{D} > 140$), this study proposes a new equation, Equation (16), to compute the static deformation, which replaces the one used in Equation (17). Therefore, by incorporating Equation (16), the expression in Equation (17) can be modified as in Equation (18) to compute the natural frequency of a long free-spanning pipeline. This new equation, Equation (18), is a hybrid of Equations (16) and (17), and therefore it is subjected to both sets of assumptions detailed here and in DNV Sect. 6.8.

$$f \approx C_1 \sqrt{\frac{EI}{m_e L_{eff}^4} \left(1 + \frac{S_{eff}}{P_{cr}} + C_3 \left(\frac{y}{D} \right)^2 \right) (1 + CSF)} \tag{18}$$

$$y_{x=\frac{L}{2}} = \frac{q_{sub}}{2 \cdot \left(\frac{q_{sub}^2 EA}{12} L_{eff}^2 \right)^3} \frac{L_{eff}^2}{2} \tag{19}$$

$$P_{cr} = (1 + CSF) \left(\frac{C_2 \pi^2 EI}{L_{eff}^2} \right) \tag{20}$$

$$CSF = k_c \left(\frac{EI_{con}}{EI_{steel}} \right)^{0.75} \tag{21}$$

$$q_{sub} = m_{sub} \cdot g = (m_s + m_c + m_f - m_{w,c}) g \tag{22}$$

where m_e is the effective mass, L_{eff} is the effective length, I is the moment of inertia for the steel pipe, E is the Young's modulus for a steel pipe, CSF is the concrete stiffness enhancement factor, D is the outer diameter of the pipe, and S_{eff} is the effective axial force, which is negative in compression. C_1 , C_2 , C_3 , and C_6 are the boundary condition coefficients, which are, respectively, 1.57, 1.0, 0.8, and 5/384 for pinned–pinned support, and 3.56, 0.25, 0.2, and 1/384 for fixed–fixed support. P_{cr} is the critical buckling load, q_{sub} is the submerged weight, k_c is the empirical constant for the deformation/slippage in the corrosion coating and the cracking of the concrete coating, and f is the cross-flow natural frequency, which becomes an in-line natural frequency when $y = 0$. Moreover, m_s , m_c , m_f , and $m_{w,c}$ are the mass of the steel pipe, the mass of the coating, the mass of the fluid (hydrogen, oil, gas, etc.), and the mass of pushed water displaced by the pipe, respectively.

In addition, according to DNV-RP-F105 Sect. 6.8 [45], the effective length of a free span can be determined using Equation (23). However, in the case of fixed–fixed support, the effective length is equivalent to the length of the pipe (i.e., $L_{eff} = L$).

$$L_{eff} = \begin{cases} 1.12 \cdot L, & \text{if } \frac{L}{D} \leq 40 \\ \left(1.12 - 0.001 \left(\frac{L}{D} - 40 \right) \right) \cdot L, & \text{if } 40 \leq \frac{L}{D} \leq 160 \\ L, & \text{if } \frac{L}{D} > 160 \end{cases} \tag{23}$$

2.3. Determination of Natural Frequency in Finite Element

As mentioned earlier, DNVGL-RP-F105 Sect. 6.8 [24] suggests utilizing the FEM for computing the responses of the long free-spanning undersea pipeline (i.e., $\frac{L}{D} > 140$). However, the FEM might be time-consuming and unsatisfied when numerous computations are required, due to the heavy graphical user interface (GUI) and complex model definition [16,44]. Consequently, in this study, the FEM-based Abaqus is used to verify the proposed closed-form solution for use in computing the static deformation and fundamental frequency of long free-span submarine pipelines.

Consequently, 212 free-span undersea pipelines are modeled (i.e., 48 models are used for the verification part and 164 for the results and discussion part) and simulated using Abaqus [46], with a two-node beam model that includes many partitions and refined mesh (i.e., one element for each meter) to speed up the simulations. During the analysis, it is important to note that different masses, i.e., submerged mass and effective mass, are employed for the static and dynamic analyses, respectively. Thus, only the effective mass, which is defined in Equation (24), is used to compute the natural frequency in Abaqus, while the positive vertical force vectors are applied to accurately determine the static displacement of the pipeline in the dynamic analysis.

$$m_e = m_s + m_c + m_f + m_{w,c} \quad (24)$$

where m_s , m_c , m_f , and $m_{w,c}$ are the mass of the steel pipe, the mass of the coating, the mass of the fluid (oil, gas, hydrogen, etc.), and the mass of pushed water displaced by the pipe and concrete, respectively. Therefore, to compute the natural frequency of the submarine pipeline in dynamic analysis, the added mass is employed to determine the effective density in terms of effective mass, which is then set as input data in Abaqus [46]. However, the effective density can result in the incorrect static deformation of the pipeline. Thus, the application of vertical upward forces on the pipeline can be utilized to rectify this issue and obtain the correct static deformation.

3. Verification

Verification of the proposed closed-form solutions is carried out by computing the static deformations and the natural frequencies of submarine pipelines with various lengths, including 10, 15, 20, 30, 40, 50, 80, 120, 140, 200, 300, and 400 m. Table 1 lists the pipeline properties and other important inputs used in the simulations. The simulations are performed with both fixed–fixed (FF) (i.e., fully clamped displacements and rotations) and pinned–pinned (PP) (i.e., fully clamped displacements and rotation above the x -axis in Abaqus) supports at both ends, while the axial force is not considered. The static deformations are computed using Equation (16), while the natural frequencies are computed using Equation (18).

Table 1. Properties for the pipeline simulation.

Input Data	Magnitude
Pipe's thickness (t)	0.015 m
Pipe's radius (r)	0.25 m
Density of the steel pipe	7850 kg/m ³
Pipe's Young modulus (E)	206 GPa
Pipe's Poisson ratio	0.3
Coating's construction strength	30 MPa
Coating's thickness	0.01 m
Density of the coating	3040 kg/m ³
Density of the seawater	1025 kg/m ³
Density of fluid inside the pipe	442.62 kg/m ³

Figures 3 and 4 illustrate comparisons of the static deformations of the free-span pipeline calculated by the present solution and the existing solutions for various magnitudes of $\frac{L}{D}$, where $D = 0.5$ m for the fixed–fixed (FF) and pinned–pinned (PP) supports, respectively. When the applied axial force and the axial forces produced by the pressure and temperature are not considered, the deformations computed by DNVGL-RP-F105 Sect. 6.8 [24] are virtually the same as those computed by Timoshenko and Goodier [47], employing the closed-form solutions as seen in Figures 3 and 4. In addition, it is somehow found that the solutions produced by Timoshenko and Goodier [47] are in reasonable agreement with those computed by the FEM for $L/D < 150$ for fixed–fixed support and $L/D < 100$ for pinned–pinned support. On the contrary, their results become significantly larger with the increase in L/D . Specifically, without an applied axial force, their results are reliable for $L/D < 160$ for fixed–fixed support and $L/D < 100$ for pinned–pinned support, and they are not reliable for the converse. On the other hand, the present solutions are in logical agreement with those computed by the FEM for a long free-span pipeline, i.e., $L/D > 160$ for FF support and $L/D > 100$ for PP support; however, they exhibit large discrepancies for the converse case, as shown in Figures 3 and 4. For example, by setting the FEM’s solution as the reference, the computed relative errors are, respectively, 49% and 21%; 56% and 694%; 57% and 178%; 62% and 54%; 93% and 19%; 170% and 3%; 670% and 20%; 1295% and 20%; 2886% and 20%; 5297% and 20%; 15,792% and 20%; and 34,128%, as calculated by the present solution, and the closed-form solutions produced by Timoshenko and Goodier [47] for $L/D = 20, 40, 60, 80, 100, 160, 240, 320, 400, 600,$ and 800 for the pinned–pinned support. Similarly, the errors in the case of fixed–fixed support for $L/D = 20, 40, 60, 80, 100, 160, 240, 320, 400, 600,$ and 800 are 20192%; 6% and 3248%; 2% and 1049%; 0.9% and 437%; 0.2% and 201%; 1.6% and 21%; 43% and 7%; 220% and 14%; 544% and 16%; 1038% and 18%; 3169% and 19%; and 6873%, as produced by the present solution and the closed-form solutions calculated by Timoshenko and Goodier [47].

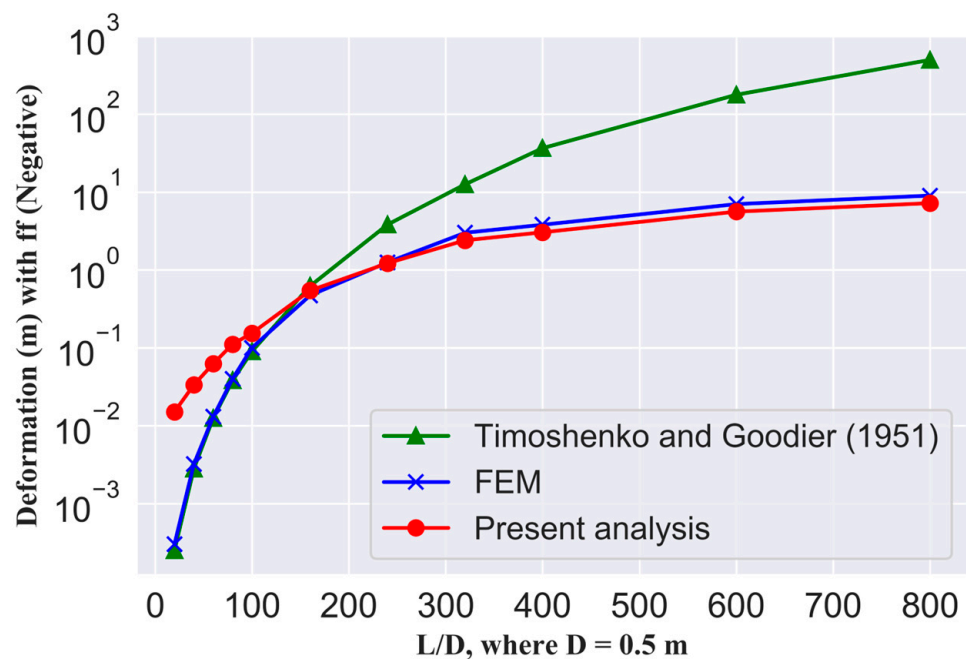


Figure 3. Comparisons of the static deformation of the free-span undersea pipeline computed by the presently proposed analysis with the solutions produced by Timoshenko and Goodier [47] and FEM [46] with various $\frac{L}{D}$ for fixed–fixed support.

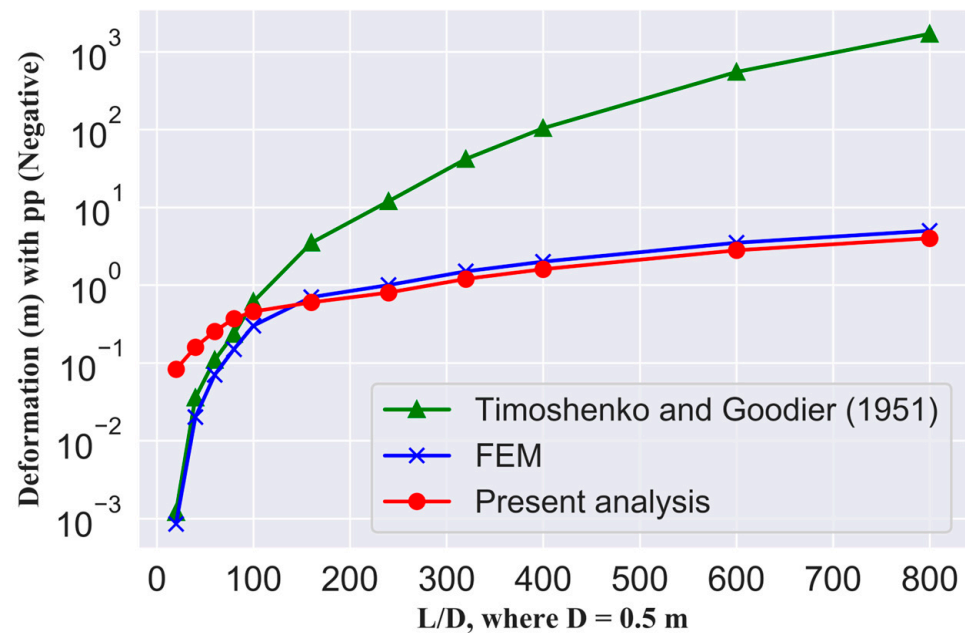


Figure 4. Comparisons of the static deformation of the free-span undersea pipeline computed by the presently proposed analysis with the solutions produced by Timoshenko and Goodier [47] and FEM [46] with various $\frac{L}{D}$ for pinned–pinned support.

Figures 5 and 6 show comparisons of the natural frequencies of the free-span pipelines calculated by the present solutions with the solutions available in the literature for the FF and PP supports, respectively. Similar to the static deformation, it is observed that the frequencies calculated by Palmer and King [12] are virtually the same as those for the in-line frequency computed by the DNVGL-RP-F105 Sect. 6.8 [24] because they neglect deformation and the applied axial force. However, Abaqus, which is based on the FEM, calculates frequency by taking into account the axial force and static deformation, leading to significantly higher frequencies than those calculated by Palmer and King [12], as seen in Figures 5 and 6. It is found that the present solutions seem reasonably agreed with the FEM's solution for a long free span; however, the differences are also reported. For instance, when using the FEM solution as a reference, the computed relative errors for the pinned–pinned supports are 19%; 19% and 18%; 20% and 17%; 21% and 20%; 28% and 28%; 39% and 44%; 63% and 46%; 73% and 49%; 81% and 51%; 86% and 52%; 91% and 52%; and 94%, produced by the present solution and Palmer and King [12], for $L/D = 20, 40, 60, 80, 100, 160, 240, 320, 400, 600$ and 800, respectively. Similarly, the computed errors for the FF support are 3%; 3% and 1%; 1% and 1%; 0.4% and 2%; 0.05% and 2%; 0.8% and 6%; 16% and 25%; 43% and 35%; 60% and 40%; 70% and 45%; 82% and 46%; and 87%, respectively.

Based on the comparison with the FEM solutions and without considering the applied axial force, it is found that the solutions of the proposed method are more reliable and reasonable than those of the existing methods when computing the static deformation and the frequency of the long free-spanning pipelines, as presented above. Additionally, the FEM-based Abaqus has been verified with closed-form solutions computed by Palmer and King [12] for $L \leq 50$ m, making its solutions reliable. Therefore, given that the analytical expression proposed in this study has been verified with the FEM solutions (as seen in Figures 3–6), it is also likely to be reliable for long free spans. This same trend is also observed for $D = 0.7$ m, as illustrated in Figures S1–S4 in the supplemental material.

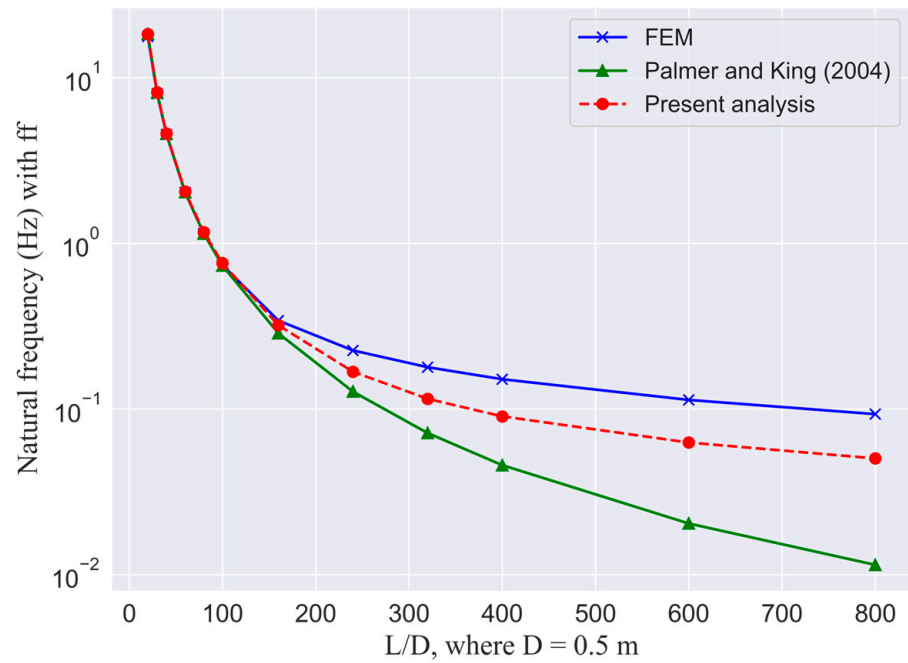


Figure 5. Comparisons of the first natural frequency of the free-spanning pipeline computed by the present solution with the solutions computed by Palmer and King [12] and FEM [46] with various $\frac{L}{D}$ for fixed–fixed support.

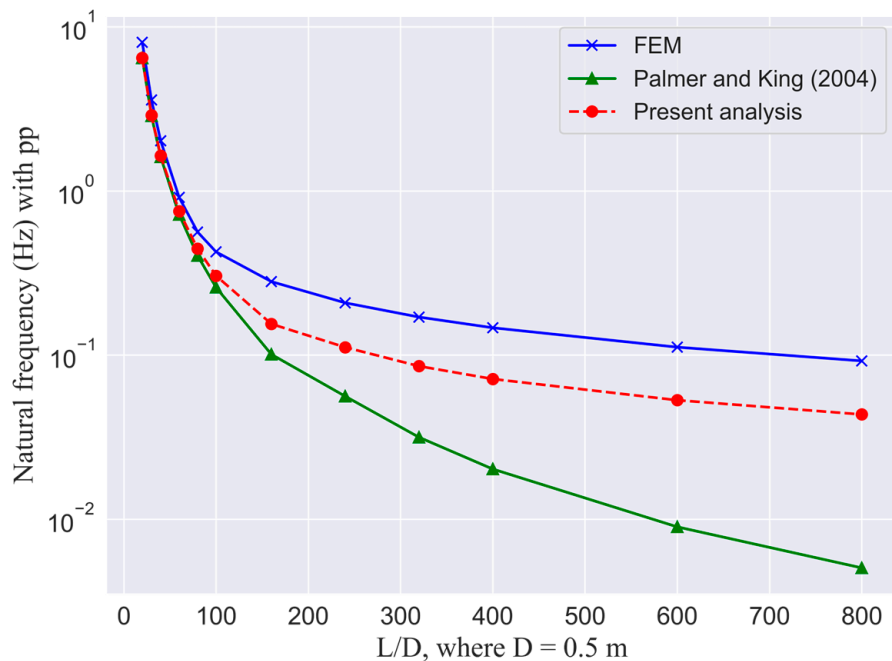


Figure 6. Comparisons of the first natural frequency of the free-spanning pipeline computed by the present solution with the solutions computed by Palmer and King [12] and FEM [46] with various $\frac{L}{D}$ for pinned–pinned support.

4. Results and Discussion

This study presents a series of simulations aimed at demonstrating the effectiveness and validity of the proposed method for computing the static deformation and natural frequency of lengthy free-span pipelines. The simulations are conducted for a range of pipeline lengths, diameters, and thicknesses. The material properties used in the simulations are taken from Table 1, except for the pipe radius and thickness. The study delves

into the influence of the pipe’s diameter on its natural frequency, which emerges from three primary factors: the self-weight of the pipe, its structural stiffness, and the displaced water, represented as an added mass. In all simulations, the supports at both ends of the pipeline are assumed to be fully clamped, with fixed–fixed (FF) supports used for all movements and pinned–pinned (PP) supports used for translation movements only.

Figure 7 compares the static deformation (Def) and first natural frequency (Freq) values of a free-spanning pipeline with $D = 0.7$ m, computed by the present solution (PS) and the FEM-based Abaqus (2021), for various combinations of length ($L = 10, 20, 50, 100, 200, 400, 600,$ and 800 m) and thickness (with D/t ratios of 10, 20, and 40) of pipe, with fixed–fixed (FF) support. As expected, the deformation values calculated by both methods gradually increase with the increasing length and thickness of the pipe. Notably, significant differences can be observed in the deformation calculated by the two methods for $L < 100$ m. However, a reasonable agreement is found for $L \geq 100$ m, as depicted in Figure 7. For instance, the relative errors computed for $L = 20, 100,$ and 800 m are 3491%, 3855%, and 3760% for $D/t = 10, 0.61%, 1.5%,$ and 12% for $D/t = 20,$ and 23%, 26%, and 36% for $D/t = 40,$ respectively.

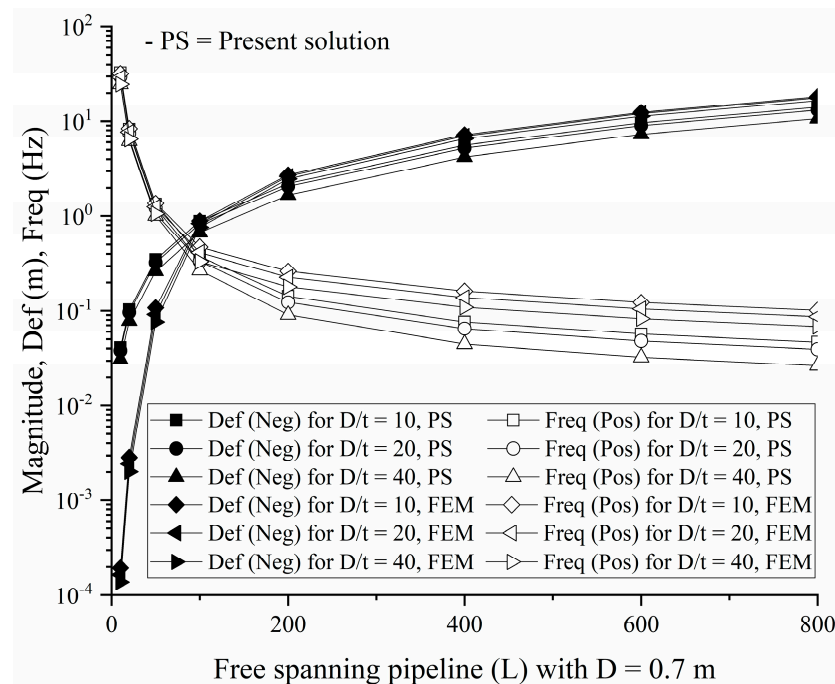


Figure 7. Comparisons of the static deformation (Def) and the first natural frequency (Freq) of the free-spanning pipelines with $D = 0.7$ m computed by the present solution (PS) and FEM-based Abaqus for the fixed–fixed support.

Similarly, the frequency of the pipeline is observed to decrease gradually as the length increases and the thickness decreases. The frequency errors computed for $D/t = 10, 20,$ and 40 are 0.9%, 2.7%, and 4.2% for $L = 20$ m, 0.6%, 1.5%, and 12% for $L = 100$ m, and 53%, 54%, and 60% for $L = 800$ m. Hence, it is evident that with FF support, the relative errors in frequency also increase gradually with the increases in the length and thickness of the pipeline.

Figures 8 and 9 present comparisons of the static deformation and frequency of the lengthy free-span pipelines for $D = 0.9$ m and $D = 1.1$ m, respectively, using the proposed method and FEM-based Abaqus for FF supports. These figures exhibit similar trends as observed for $D = 0.7$ m, demonstrating the validity and effectiveness of the proposed method for various pipe diameters. The frequency values calculated by this method for various diameters with a constant D/t ratio and length of 800 m show negligible differences. For example, with $D/t = 40,$ the frequency values computed by the proposed method for

$D = 0.7$ m, 0.9 m, and 1.1 m are 0.027 Hz, 0.026 Hz, and 0.026 Hz, respectively. Similarly, for $D/t = 20$, the frequencies calculated by the proposed method for $D = 0.7$ m, 0.9 m, and 1.1 m are 0.0393 Hz, 0.0394 Hz, and 0.0396 Hz, respectively. Therefore, it can be concluded that the increase in pipe diameter with a constant D/t ratio has a negligible effect on the frequency of a long free-spanning submarine pipeline with FF support.

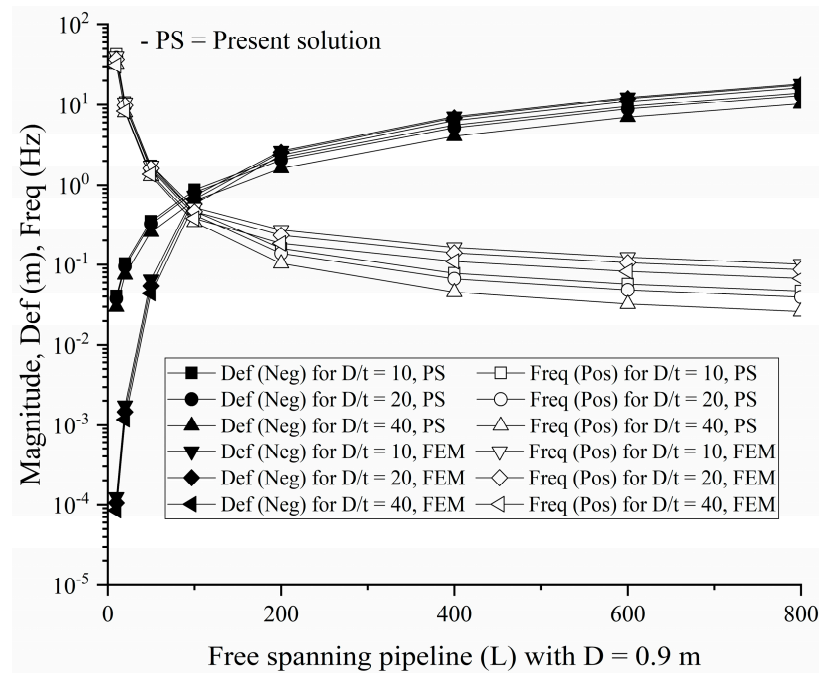


Figure 8. Comparisons of the static deformation (Def) and the first natural frequency (Freq) values of a free-spanning pipelines with $D = 0.9$ m computed by the present solution (PS) and FEM-based Abaqus for fixed–fixed support.

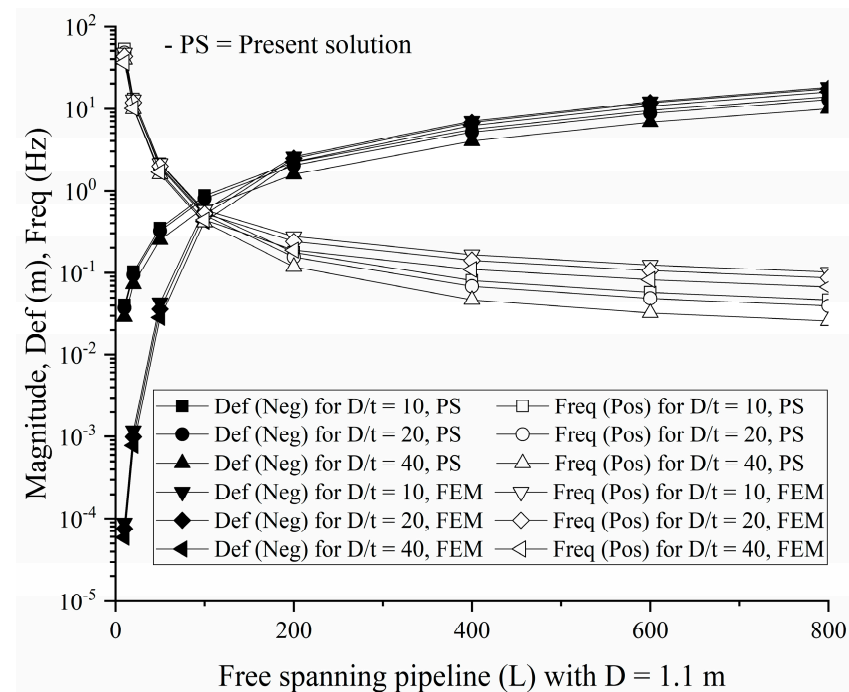


Figure 9. Comparisons of the static deformation (Def) and the first natural frequency (Freq) values of free-spanning pipelines with $D = 1.1$ m computed by the present solution (PS) and FEM-based Abaqus for fixed–fixed support.

Figures 10–12 illustrate comparisons between the present solution (PS) and the FEM-based solution [46] as regards the first natural frequency (Freq) and static deformation (Def) of a free-spanning pipeline with pinned–pinned support and different combinations of thickness and length of pipe, with diameters of $D = 0.7, 0.9,$ and 1.1 m, respectively. The results show that, in general, the deformation increases with increasing thickness and length of the pipeline, while the frequency decreases with increasing length and thickness.

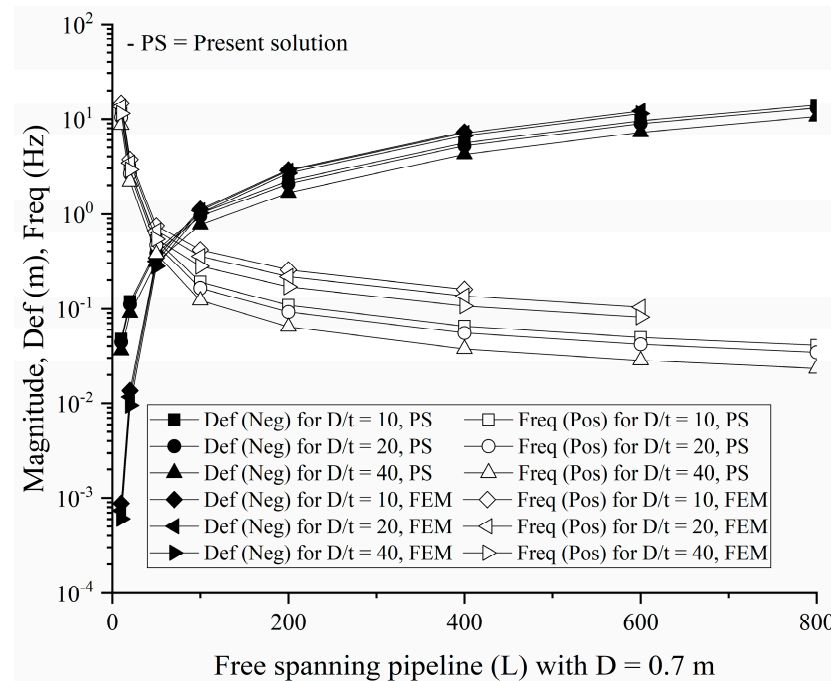


Figure 10. Comparisons of the static deformation (Def) and the first natural frequency (Freq) values of free-spanning pipelines with $D = 0.7$ m computed by the present solution (PS) and FEM-based Abaqus for pinned–pinned support.

Furthermore, Figures 10–12 demonstrate that, with pinned–pinned support, the deformation and frequency of the free-spanning pipeline computed using the present solution (PS) and FEM [46] show a reasonable agreement at $L \geq 100$ m, while a large difference is found at $L < 100$ m. Notably, simulating a pipeline with a small diameter and a large thickness using FEM is challenging due to the pipeline’s excessive self-weight (Figures 10 and 11); however, the proposed method can overcome this difficulty with reasonable solutions, thanks to its analytical approach. Therefore, the present solution (PS) can be used to compute the deformations and frequencies of a pinned–pinned-supported pipeline, as shown in Figures 10–12. Similar to the FF support case of a long free-spanning underwater pipeline, the increase in pipeline diameter with a constant D/t ratio has virtually no effect on the frequency computed for the PP support.

By and large, the frequency of PP supports is found to be significantly lower than that of FF supports with a short span. However, there is hardly any difference in frequency between the two supports with a long span, as mentioned earlier. It should be noted that the proposed method does not aim to provide an exact solution for the static deformation and natural frequency in comparison to the FEM solutions [46]. Nonetheless, it yields more reasonable solutions than the existing ones—especially when compared to the FEM solution [46]—for a long free-spanning submarine pipeline in the absence of applied axial forces.

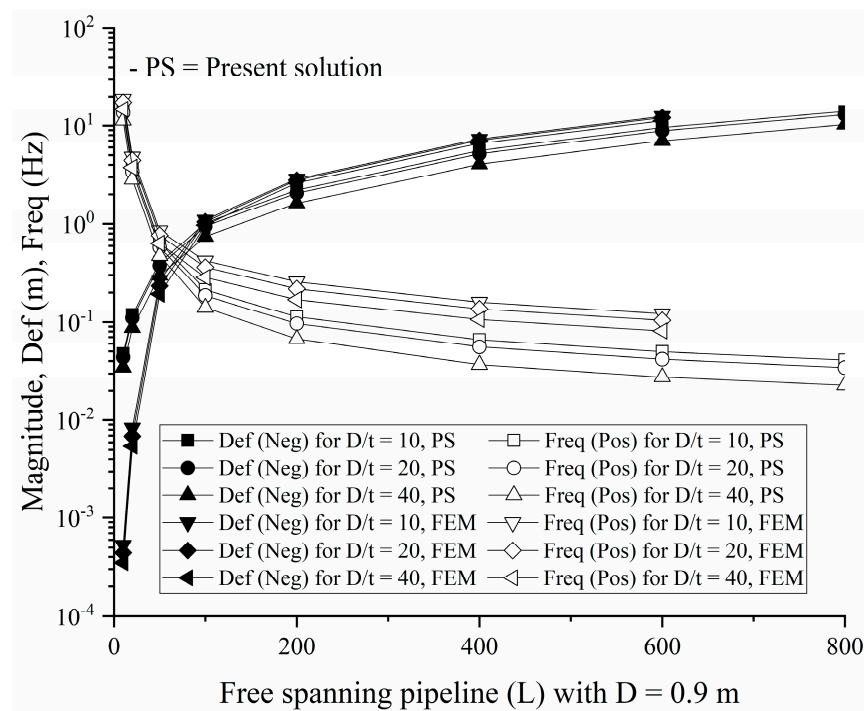


Figure 11. Comparisons of the static deformation (Def) and first natural frequency (Freq) values of free-spanning pipelines with $D = 0.9$ m computed by the present solution (PS) and FEM-based Abaqus for pinned–pinned support.

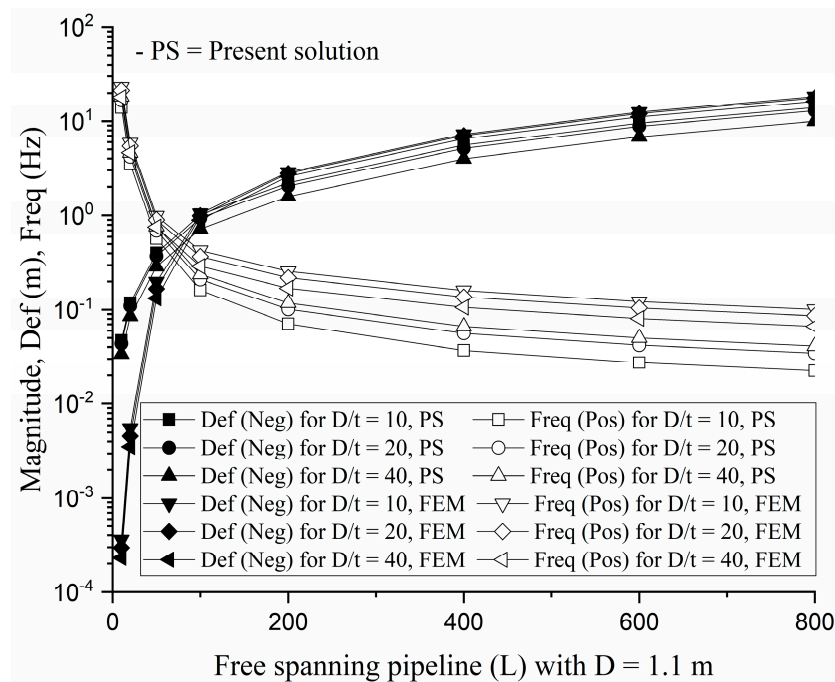


Figure 12. Comparisons of the static deformation (Def) and first natural frequency (Freq) values of free-spanning pipelines with $D = 1.1$ m computed by the present solution (PS) and FEM-based Abaqus for pinned–pinned support.

5. Conclusions

A new closed-form solution for computing the approximated static deformation and the fundamental natural frequency of a long free-span underwater pipeline was developed by employing the energy method-based cable theory in conjunction with the analytical

solution produced by DNVGL-RP-F105 Sect. 6.8 [24] (see Equation (18)). The proposed analytical solution is straightforward to implement for long free pipelines and has not been reported in the literature. To verify the proposed method, the static displacement and frequency values for different pipeline lengths (i.e., $L = 10, 15, 20, 30, 40, 50, 80, 120, 140, 200, 300,$ and 400 m) were computed and compared with those calculated using the FEM-based Abaqus (2021), and they show better agreement than the existing solutions. For instance, with $L/D = 100$ to 800 and using the FEM solution as a reference, the computed relative errors do not reach 20% for deformation and 50% for frequency for both pinned–pinned and fixed–fixed supports. Additionally, the proposed method was successfully implemented to compute the deformation and frequency for long free-spanning undersea pipelines with various combinations of lengths (i.e., $L = 10, 20, 50, 100, 200, 400, 600$ and 800 m), thicknesses (which have ratio $D/t = 10, 20,$ and 40) and diameters (i.e., $D = 0.7, 0.9$ and 1.1 m).

It should be noted that DNVGL-RP-F105 Sect. 6.8 [24] provides an unreliable frequency, yielded by the inaccurately calculated deformation of the pipe for $L/D \geq 140$, where L and D denote the length and diameter of the pipeline, respectively. Therefore, this study extends the method proposed in DNVGL-RP-F105 Sect. 6.8 [24] to provide reliable frequency calculations for $L/D \geq 140$. Specifically, the current method provides reliable deformation for $L/D \geq 100$. Furthermore, it is evident that, when static deformation is not taken into account in the dynamic analysis, the cross-flow natural frequency equals the in-line natural frequency. Consequently, the in-line frequency is equivalent to the frequency calculated by the closed-form solution (e.g., Palmer and King [12]).

In summary, the key findings reveal that longer pipelines have a lower frequency due to the increase in length. Consequently, the diameter-to-thickness ratio (D/t) and the increase in pipeline deformation have minimal effects on the fundamental frequency of long free-spanning submarine pipelines. Furthermore, regarding support type, FF supports yield a significantly higher frequency for short spans, but for long spans, the frequencies are comparable. For example, for $L/D = 800$, the discrepancy between the FF and PP supports is around 10%. It is important to note that this new method offers more reasonable solutions compared to existing ones, especially for $L/D > 140$, which has not previously been addressed. This could aid in mitigating vortex-induced vibration (VIV) in the preliminary design of long free-spanning submarine pipelines.

Supplementary Materials: The following supporting information can be downloaded at: <https://www.mdpi.com/article/10.3390/math11214481/s1>, Figure S1. Comparisons of the static deformation of the free-span submarine pipelines computed by the present analysis with the existing solutions for various L/D , where $D = 0.7$ for fixed–fixed support. Figure S2. Comparisons of the static deformation of the free-span submarine pipelines computed by the present analysis with the existing solutions for various L/D , where $D = 0.7$ for pinned–pinned support. Figure S3. Comparisons of the natural frequency of the free-span submarine pipelines computed by the present analysis with the existing solutions for various L/D , where $D = 0.7$ for fixed–fixed support. Figure S4. Comparisons of the natural frequency of the free-span submarine pipelines computed by the present analysis with the existing solutions for various L/D , where $D = 0.7$ for pinned–pinned support.

Author Contributions: Writing—original draft preparation, T.P.; writing—review and editing, T.P., A.G. and P.A.T.; visualization, T.P., A.G. and P.A.T.; supervision, A.G. and P.A.T.; project administration, A.G. and P.A.T.; funding acquisition, A.G. and P.A.T. All authors have read and agreed to the published version of the manuscript.

Funding: This research received no external funding.

Data Availability Statement: The datasets generated and/or analyzed in the present study are available from the corresponding author upon reasonable request.

Acknowledgments: The support from Israel’s Ministry of Energy (grant number 220-17-007) is gratefully acknowledged.

Conflicts of Interest: The authors declare no conflict of interest.

Nomenclature

A	cross-section area of the pipe
C_1	boundary condition coefficient (1.57 for pinned–pinned support and 3.56 for fixed–fixed support)
C_2	boundary condition coefficient (1.0 for pinned–pinned support and 0.25 for fixed–fixed support)
C_3	boundary condition coefficient (0.8 for pinned–pinned support and 0.2 for fixed–fixed support)
C_6	boundary condition coefficient (5/384 for pinned–pinned support and 1/384 for fixed–fixed support)
CSF	concrete stiffness enhancement factor
D	outer diameter of pipe
dx	infinitesimal change of pipeline in x direction
dy	infinitesimal change of pipeline in y direction
E	Young’s modulus
f	natural frequency
g	acceleration of gravity
H	constant horizontal force
h	different level of the pipeline supports
I	moment of inertia of steel pipe
k	constant stiffness
k_c	empirical constant
L	length of pipeline
L_{eff}	effective length
m_c	mass of coating
m_e	effective mass
m_f	mass of fluid
m_s	mass of steel pipeline
$m_{w.c}$	mass of displaced water
P_{cr}	critical buckling load of pipeline
q_{sub}	submerged weight
q	uniformly distributed load
r	radius of pipe
S_{eff}	effective axial force
T	axial force generated by configuration shape of pipeline
U	strain energy
ν	Poisson’s ratio of steel pipe
v_1	vertical force at point 1
v_2	vertical force at point 2
W	virtual work done
x	variable length of pipeline
y	static deformation of pipeline
δ	static deformation of pipeline

References

1. Choi, H.S. Free Spanning Analysis of Offshore Pipelines. *Ocean Eng.* **2001**, *28*, 1325–1338. [[CrossRef](#)]
2. Vedeld, K.; Sollund, H.; Hellesland, J. Free Vibrations of Free Spanning Offshore Pipelines. *Eng. Struct.* **2013**, *56*, 68–82. [[CrossRef](#)]
3. Gullaksen, J. Implementation of a Method for Free-Spanning Pipeline Analysis. In Proceedings of the International Conference on Offshore Mechanics and Arctic Engineering—OMAE, Virtual, Online, 21–30 June 2021; American Society of Mechanical Engineers (ASME): New York, NY, USA, 2021; Volume 4.
4. Anfinson, K.A. Review of Free Spanning Pipelines. In Proceedings of the International Offshore and Polar Engineering Conference, The Hague, The Netherlands, 11–16 June 1995; International Society of Offshore and Polar Engineers: Mountain View, CA, USA, 1995; pp. 129–133.
5. Bao, R.D.; Wen, B.C. Dynamic Response Analysis of Submarine Free Spanning Pipeline. *Zhendong yu Chongji/J. Vib. Shock* **2007**, *26*, 140–143.

6. Georgiadou, S.; Loukogeorgaki, E.; Angelides, D.C. Dynamic Analysis of a Free Span Offshore Pipeline. In Proceedings of the International Offshore and Polar Engineering Conference, Busan, Republic of Korea, 15–20 June 2014; International Society of Offshore and Polar Engineers: Mountain View, CA, USA, 2014; pp. 80–87.
7. Barrette, P. Offshore Pipeline Protection against Seabed Gouging by Ice: An Overview. *Cold Reg. Sci. Technol.* **2011**, *69*, 3–20.
8. Rumson, A.G. The Application of Fully Unmanned Robotic Systems for Inspection of Subsea Pipelines. *Ocean Eng.* **2021**, *235*, 109214. [[CrossRef](#)]
9. Phuor, T.; Potty, N.S.; Akram, M.K.M. Mathematical Matrix Method to Predict Project Total Cost & Schedule. *Int. J. Appl. Eng. Res.* **2014**, *9*, 5029–5056.
10. Phuor, T. Prediction of the Total Cost and Monitoring and Control of Offshore Pipework Project Using the Integrated Mathematical Matrix Method. Master's Thesis, Civil Engineering Department, Universiti Teknologi PETRONAS, Seri Iskandar, Malaysia, 2015.
11. Trapper, P.A. Feasible Numerical Analysis of Steel Lazy-Wave Riser. *Ocean Eng.* **2020**, *195*, 106643. [[CrossRef](#)]
12. Palmer, A.C.; King, R.A. *Subsea Pipeline Engineering*; PennWell: Tulsa, OK, USA, 2004; Volume 53, ISBN 1593701330.
13. Trapper, P.A.; Mishal, I. Numerical Analysis of Offshore Pipe-Lay Subjected to Environment-Induced Non-Uniformly Distributed Follower Loads. *Appl. Ocean Res.* **2020**, *100*, 102149. [[CrossRef](#)]
14. Elost, H.; Huang, S.; Incecik, A. Wave Loading Fatigue Reliability and Uncertainty Analyses for Geotechnical Pipeline Models. *Ships Offshore Struct.* **2014**, *9*, 450–463. [[CrossRef](#)]
15. Elost, H.; Huang, S.; Incecik, A. Seabed Interaction Modeling Effects on the Global Response of Catenary Pipeline: A Case Study. *J. Offshore Mech. Arct. Eng.* **2014**, *136*, 032001. [[CrossRef](#)]
16. Trapper, P.A. A Numerical Model for Geometrically Nonlinear Analysis of Long Free Spanning Offshore Pipelines Enhanced with Buoyancy Modules. *Appl. Ocean Res.* **2022**, *124*, 103224. [[CrossRef](#)]
17. Trapper, P.A. A Numerical Model for Geometrically Nonlinear Analysis of a Pipe-Lay on a Rough Seafloor. *Ocean Eng.* **2022**, *252*, 111146. [[CrossRef](#)]
18. Sun, J.; Huang, S. *Pipeline Spanning*; Wiley: Hoboken, NJ, USA, 2017.
19. Trapper, P.A. Static Analysis of Offshore Pipe-Lay on Flat Inelastic Seabed. *Ocean Eng.* **2020**, *213*, 107673. [[CrossRef](#)]
20. Bai, Q.; Bai, Y. *Subsea Pipeline Design, Analysis, and Installation*; Elsevier Inc.: Amsterdam, The Netherlands, 2014.
21. Trapper, P.A. Feasible Numerical Method for Analysis of Offshore Pipeline in Installation. *Appl. Ocean Res.* **2019**, *88*, 48–62. [[CrossRef](#)]
22. Kim, D.K.; Incecik, A.; Choi, H.S.; Wong, E.W.C.; Yu, S.Y.; Park, K.S. A Simplified Method to Predict Fatigue Damage of Offshore Riser Subjected to Vortex-Induced Vibration by Adopting Current Index Concept. *Ocean Eng.* **2018**, *157*, 401–411. [[CrossRef](#)]
23. Liu, G.; Li, H.; Xie, Y.; Incecik, A.; Li, Z. Investigating Cross-Flow Vortex-Induced Vibration of Top Tension Risers with Different Aspect Ratios. *Ocean Eng.* **2021**, *221*, 108497. [[CrossRef](#)]
24. *DNVGL-RP-F105*; Recommended Practice: Free Spanning Pipelines. DNV: Bærum, Norway, 2017.
25. Gvirtzman, Z.; Reshef, M.; Buch-Leviatan, O.; Groves-Gidney, G.; Karcz, Z.; Makovsky, Y.; Ben-Avraham, Z. Bathymetry of the Levant Basin: Interaction of Salt-Tectonics and Surficial Mass Movements. *Mar. Geol.* **2015**, *360*, 25–39. [[CrossRef](#)]
26. Xiao, Z.; Zhao, X. Prediction of Natural Frequency of Free Spanning Subsea Pipelines. *Int. J. Steel Struct.* **2010**, *10*, 81–89. [[CrossRef](#)]
27. Beckmann, M.M.; Hale, J.R.; Lamison, C.W. Spanning Can Be Prevented, Corrected in Deeper Water. *Oil Gas J.* **1991**, *89*, 84–89.
28. White, F. *Viscous Fluid Flow*, 3rd ed.; McGraw Hill: New York, NY, USA, 2006.
29. Tu, J.; Yeoh, G.H.; Liu, C. *Computational Fluid Dynamics: A Practical Approach*; Elsevier: Amsterdam, The Netherlands, 2018.
30. Qian, Y.; Wang, S.; Chen, S. Multi-Frequency Homotopy Analysis Method for Coupled Van Der Pol-Duffing System with Time Delay. *Mathematics* **2023**, *11*, 407. [[CrossRef](#)]
31. Qiang, Y.H.; Qian, Y.H.; Guo, X.Y. Periodic Solutions of Delay Nonlinear System by Multi-Frequency Homotopy Analysis Method. *J. Low Freq. Noise Vib. Act. Control* **2019**, *38*, 1439–1454. [[CrossRef](#)]
32. Liu, Y.Y.; Hao, Y.X.; Zhang, W.; Liu, L.T.; Yang, S.W.; Cao, Y.T. Frequency Veering of Rotating Metal Porous Twisted Plate with Cantilever Boundary Using Shell Theory. *Acta Mech. Solida Sin.* **2022**, *35*, 282–302. [[CrossRef](#)]
33. Yang, S.W.; Hao, Y.X.; Zhang, W.; Ma, W.S.; Wu, M.Q. Nonlinear Frequency and Bifurcation of Carbon Fiber-Reinforced Polymer Truncated Laminated Conical Shell. *J. Vib. Eng. Technol.* **2023**. [[CrossRef](#)]
34. Mao, J.J.; Guo, L.J.; Zhang, W. Vibration and Frequency Analysis of Edge-Cracked Functionally Graded Graphene Reinforced Composite Beam with Piezoelectric Actuators. *Eng. Comput.* **2023**, *39*, 1563–1582. [[CrossRef](#)]
35. Yaghoobi, M.; Mazaheri, S.; Jabbari, E. Determining Natural Frequency of Free Spanning Offshore Pipelines by Considering the Seabed Soil Characteristics. *J. Persian Gulf* **2012**, *3*, 25–33.
36. Sarkar, G.; Roy, P. Influence of Seabed Soil Characteristics on Eigenfrequency of Offshore Free Spanning Pipeline. In *Proceedings of the Lecture Notes in Civil Engineering*; Springer: Singapore, 2020; Volume 92.
37. Sarkar, G.; Roy, P. Effect of Non-Homogeneity of Seabed Soil on Natural Frequency of Offshore Free Spanning Pipeline. In *Proceedings of the Lecture Notes in Civil Engineering*; Springer: Singapore, 2022; Volume 188.
38. Energean. *Karish and Tanin Field Development Plan*; Energean: London, UK, 2017.
39. Phuor, T.; Ganz, A.; Trapper, P.A. Bearing Capacity Factors of the Cone-Shaped Footing in Meshfree. *Int. J. Numer. Anal. Methods Geomech.* **2022**, *47*, 275–298. [[CrossRef](#)]

40. Phuor, T.; Harahap, I.S.; Ng, C.-Y. Bearing Capacity Factors of Flat Base Footing by Finite Elements. *ASCE J. Geotech. Geoenviron. Eng.* **2022**, *148*, 04022062. [[CrossRef](#)]
41. Phuor, T. Development and Application of Three-Dimensional Finite Element Interface Model for Soil-Jack-Up Interaction during Preloading. Ph.D. Thesis, Civil Engineering Department, Universiti Teknologi PETRONAS, Seri Iskandar, Malaysia, 2020.
42. Gong, S.; Xu, P.; Bao, S.; Zhong, W.; He, N.; Yan, H. Numerical Modelling on Dynamic Behaviour of Deepwater S-Lay Pipeline. *Ocean Eng.* **2014**, *88*, 393–408. [[CrossRef](#)]
43. Jiwa, M.Z.; Kim, D.K.; Mustaffa, Z.; Choi, H.S. A Systematic Approach to Pipe-in-Pipe Installation Analysis. *Ocean Eng.* **2017**, *142*, 478–490. [[CrossRef](#)]
44. Guo, B.; Song, S.; Ghalambor, A.; Tian Ran, L. *Offshore Pipelines: Design, Installation, and Maintenance*; Gulf Professional Publishing: Houston, TX, USA, 2014.
45. Det Norske Veritas. *Guidelines 14. Free Spanning Pipelines*; Det Norske Veritas: Bærum, Norway, 1998.
46. Abaqus. Abaqus Version 2021-1 Analysis User's Manual. 2021. Available online: <https://www.3ds.com/> (accessed on 9 September 2023).
47. Timoshenko, S.; Goodier, J.N. *Theory of Elasticity*; McGRAW-HILL: New York, NY, USA, 1951.

Disclaimer/Publisher's Note: The statements, opinions and data contained in all publications are solely those of the individual author(s) and contributor(s) and not of MDPI and/or the editor(s). MDPI and/or the editor(s) disclaim responsibility for any injury to people or property resulting from any ideas, methods, instructions or products referred to in the content.